ELSEVIER

Chemical Engineering Journal 80 (2000) 23–30

Chemical Engineering Journal

www.elsevier.com/locate/cej

The structure and strength of depletion force induced particle aggregates

Yao-de Yan*, Janine L. Burns, Graeme J. Jameson, Simon Biggs

Centre for Multiphase Processes, Department of Chemical Engineering and Department of Chemistry, The University of Newcastle, Callaghan, NSW 2308, Australia

Abstract

Aggregating fine particulate matter is common practice in many industrial solid-liquid separation processes. Data obtained in this work on dilute aqueous dispersions of model colloidal polystyrene latex spheres indicate that depletion flocculation, which uses non-adsorbing polymer, can yield very compact aggregates. Flocculation of the negatively charged latex particles was induced by the addition of a poly(acrylic acid) at pH 10. The structural compactness of the latex flocs formed in the dilute dispersions was characterised using small-angle static light scattering in terms of mass fractal dimensions. Rheological measurements on the concentrated latex dispersions in the presence of the non-adsorbing polyacid showed Bingham yield stress behaviour. Both the compactness and strength of the latex flocs were found to be significantly dependent upon the level of the polyacid, as well as the concentration of the initial particles. In particular, as the level of the polyacid was raised the floc compactness decreased, whereas its strength increased. They were both seen to level off at high polymer concentrations. Atomic force microscopy measurements were made at varying concentrations of the polyacid to provide a qualitative explanation of the observed floc structural behaviour of the dilute dispersions. By combining the fractal dimension and the Bingham yield stress we were also able to estimate the energy required to separate the flocs into single units in the concentrated dispersions. It was concluded that the interparticle interaction energy is the key to understanding the dependence of both the floc structure and strength on the polymer concentration.

Keywords: Depletion flocculation; Mass fractal aggregates; Floc strength; Small-angle static light scattering; Atomic force microscopy

1. Introduction

An understanding of the aggregation processes of fine particles is of fundamental importance in colloid, material, biological and environmental sciences. It also has wide implications in many industrial solid-liquid separation processes such as thickening, settling, filtration or flotation, where solids separation efficiency is enhanced with the increased size of the resultant aggregates. Different applications may, however, require aggregates of differing characteristics [1]. For instance, in applications where solids consolidation is the main objective, aggregates possessing higher mass densities are desired, since low density aggregates are voluminous due to high solvent content.

The majority of industrial processes involve aqueous dispersions whose stability is controlled by the presence of some surface charge on the constituent particles which results in the DLVO-type electric double layer repulsion [2]. The suppression of this stabilising effect can easily be achieved, for example, by the addition of moderate amounts of a simple inert electrolyte [3,4]. Destabilisation can also be induced by adding a polymeric flocculant [5] which either adsorbs to the particle surface (bridging flocculation) or is non-adsorbing (depletion flocculation). Salt-induced particle coagulation and in particular polymer-induced bridging flocculation are currently the most common mechanisms being employed in industrial applications.

Knowing the structure of aggregates is vital if one wishes to better understand and control the aggregation process. Since the advent of fractal mathematics in the mid 1970s [6], fractal techniques have been increasingly applied to the aggregate structural analysis. It is now known that aggregates formed from random aggregation processes are generally mass fractals, meaning that the aggregate structure is scale invariant. In the theory of mass fractals the mass fractal dimension, D, corresponds to the degree of irregularity or the space-filling capacity of an object. D is related to the mass density, $\rho(R)$, of an aggregate of radius R by

$$\rho(R) \propto R^{D-3} \tag{1}$$

Hence, D is a good measure of the structural compactness of an aggregate. In three-dimensional Euclidean space

* Corresponding author. Tel.: +61-2-49216181; fax: +61-2-49601445.
E-mail address: cgyy@cc.newcastle.edu.au (Y.-d. Yan).

1383-5866/00/$ – see front matter
PII: S1383-5866(00)00073-3

D ranges from 1 for tenuous aggregates to 3 for totally compacted material.

In salt-induced perikinetic aggregation processes the aggregate mass fractal dimension generally ranges from 1.75 for diffusion-limited cluster-cluster aggregation at high salt concentrations to 2.1 for reaction-limited cluster-cluster aggregation at low salt concentrations [3,4,7]. In comparison, the structural aspects of polymer bridging flocculated aggregates are less well known. There has been some experimental [8–10] and computer simulation work [11,12] which indicates that the mass fractal dimension of such aggregates ranges from 1.7 to 2.5. The aggregate structure was found to be strongly dependent on the molecular weight, charge density (in the case of a polyelectrolyte) and conformation of the polymer used.

It has long been observed that when a colloidal dispersion is mixed with a polymer that does not adsorb onto the particle surfaces, phase separation into particle-rich and polymer-rich phases can occur [13,14]. This is widely known as polymer-induced depletion flocculation. Asakura and Oosawa [15] were the first to predict theoretically the depletion phenomena. Depletion interactions can generally be understood as follows (cf. Fig. 1): There is a segmental concentration gradient of a polymer coil in the vicinity of a particle surface such that the polymer concentration is essentially zero at the particle surface and increases to the bulk value. The distance over which this interaction occurs is known as the depletion layer thickness, which in reality can be approximated by the radius of gyration of the polymer coil. Upon close approach of two colloidal particles, each having a depletion layer, polymer segments from the dilute region between the particles are forced out into the more concentrated bulk solution, thus leaving behind a reservoir of pure solvent between the particles. This creates an osmotic pressure gradient and hence an attractive force between the particles. It should be noted that the depletion layer thickness and the osmotic pressure act in opposite directions: Increasing the polymer concentration leads to a rise in the osmotic pressure and a decrease in the depletion layer thickness.

Almost all existing work on depletion flocculation has focussed on the phase behaviour of such systems. Very little is known about the structure of aggregates that are formed from this flocculation mechanism. Two studies [16,17] have appeared in the literature which deal with the structural aspects of depletion induced flocs, with both using the small-angle static light scattering technique. Burns et al. [17] monitored the flocculation behaviour of very dilute aqueous dispersions of colloidal polystyrene latex spheres in the presence of a non-adsorbing poly(acrylic acid), whereas Poon et al. [16] studied the depletion phenomena of concentrated non-aqueous dispersions of coated PMMA spheres. Both investigations revealed the fractal nature of the particle flocs. Values for the floc mass fractal dimension from 1.7 up to 3 were obtained. These studies show the possibility that very high *D* values and therefore very compact aggregates can be obtained through depletion flocculation.

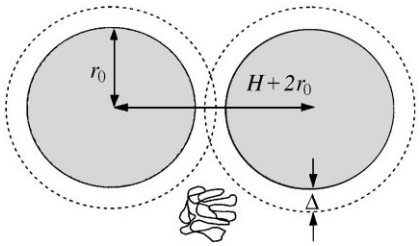

Fig. 1. A schematic illustration of polymer depletion between two approaching particles of equal size, each having a polymer depletion layer thickness of Δ.

This paper presents an experimental study on the structure and strength of depletion-induced flocs. Our aim is to provide a qualitative understanding of the observed floc characteristics on the basis of interparticle interaction energy. Colloidal-sized polystyrene latex spheres were used as the primary particles. These latices are particularly useful model particles for aggregation studies, since they can be prepared with controlled sizes and low polydispersity. Their neutral buoyancy in water also reduces problems associated with particle settling during extended experimental periods. Depletion flocculation of the latex particles was induced by the addition of a poly(acrylic acid) at a high solution pH. Structural compactness of the flocs was examined with the small-angle static light scattering technique, whereas floc strength was obtained from rheometry. Information about the interparticle interaction energy was derived from atomic force microscopy and rheological measurements.

2. Experimental

2.1. Latex particles and poly(acrylic acid)

The primary polystyrene latex spheres used in this work were synthesised according to the surfactant-free emulsion polymerisation method of Goodwin et al. [18] using styrene monomer and ammonium persulphate as the initiator. After synthesis, the particles were thoroughly dialysed against Millipore water. Details of the preparation and characterisation procedures can be found in Ref. [7]. Transmission electron microscopy yielded a particle radius of 165±5 nm. The particles carried negative surface charges and their surface functional groups were found to be fully ionised above pH 6.

Poly(acrylic acid) (or PAA) with a nominal molecular weight of 250 000 g mol^{-1} was purchased from Aldrich and used as supplied. It is estimated that the pK_a of a high molecular weight polyacid is around 5. Above pH 5 more than 50% of the functional groups along the polyacid chain will be ionised.

2.2. Depletion flocculation

Adsorption tests were carried out as a function of the aqueous solution pH (adjusted using KOH and HNO_3) to ensure

that under the solution conditions used in the subsequent flocculation work no adsorption of the polyacid onto the latex particle surfaces occurred. This was done by mixing the PAA solutions at a range of concentrations with a fixed volume of latex particles and tumbling at 25°C for 24 h. After settling out of the particles by centrifugation the equilibrium concentration of PAA in the supernatant was analysed using a spectrofluorimetric technique [19]. The results indicate that there was no measurable adsorption of the polyacid at pH $\geq$7. As a result, the solution pH of all the flocculation tests reported in the subsequent sections was maintained at 10.

2.3. Probing floc structure with small-angle static light scattering

Small-angle static light scattering is well suited for the study of aggregate structures in dilute dispersions. For a mass fractal aggregate consisting of monodisperse primary particles and satisfying the criteria of the Rayleigh–Gans–Debye regime, there exists a simple power-law scattering relation [20] between the scattered intensity from the aggregate, $I(Q)$, and the magnitude of the scattering wavevector, Q, i.e.

$$I(Q) \propto Q^{-D} \tag{2}$$

provided that $1/R << Q << 1/r_0$, where R and r_0 are the respective radii of the aggregate and the primary particles. The magnitude of the scattering wavevector is defined as $Q = 4\pi n_0 \sin(\theta/2)/\lambda_0$, where n_0 is the refractive index of the dispersion medium, θ is the scattering angle and λ_0 is the in vacuo wavelength of the incident light. Since $1/Q$ is the length scale probed in a scattering experiment, the low and high regions of Q reveal, respectively, the overall structure of the aggregate and the structure of the constituent primary particles. The spatial arrangement of the primary particles inside an aggregate can only be probed when $1/R \ll Q \ll 1/r_0$. Eq. (2) is the basis for determining the mass fractal dimension of aggregates from scattering techniques.

The Mastersizer S (Malvern Instruments, UK) with a 632.8 nm He–Ne laser was used for the scattering work on our dilute latex dispersions. This instrument provides a simultaneous measurement of scattered intensities from the aggregating sample at a range of scattering angles (0–46°). The aggregating sample in the scattering cell was monitored as a function of time under perikinetic conditions. When the size of the aggregates was sufficiently larger than that of the primary particles, the log $I(Q)$ versus log Q plot was used to determine the mass fractal dimension of the aggregates. Typical average diameters of our depletion-induced latex aggregates were 3–5 μm.

2.4. Measuring floc strength with rheometry

In weakly flocculated colloidal dispersions the Bingham yield stress (τ_B), which is a measure of floc strength and corresponds to the maximum force per unit area that the floc structure can withstand before rupturing, can be related to the energy (E_{sep}) required to separate the flocs into single units [21–24], i.e.

$$\tau_B = 3\phi_s n E_{sep}/(8\pi r_0^3) \tag{3}$$

where ϕ_s is the volume fraction of the primary particles in the dispersion, n is the average number of contacts per particle in the floc (i.e. the coordination number), and r_0 is the radius of the primary particles. Although the real situation can be significantly more complex, Eq. (3) shows the inherent relationship between the floc microstructure (n), strength (τ_B) and the force or energy (E_{sep}) existing amongst the primary particles.

The steady-state shear stress (τ) and shear rate ($\dot{\gamma}$) relation of the concentrated latex dispersions in the presence of the non-adsorbing polyacid was measured on a Bohlin CVO constant shear stress rheometer. The instrument uses a concentric cylinder configuration. The gap width between the two cylinders is 1.25 mm and the outer cylinder is stationary. The Bingham yield stress was obtained from the intercept by extrapolation of the linear portion of the τ–$\dot{\gamma}$ curve to $\dot{\gamma}=0$. All measurements were performed at pH 10 and 25°C. Prior to a measurement each sample was pre-sheared for 10 min. The pre-shear stress was chosen to be considerably higher than the yield stress of each dispersion. The sample was then left to flocculate for 10 min in the rheometer. A shear stress sweep was then applied to obtain the relevant τ–$\dot{\gamma}$ curve.

2.5. Direct force measurements with atomic force microscopy

To better understand the properties of depletion-induced particle flocs it is invaluable to gain information about the interaction forces between the primary particles. Atomic force microscopy (AFM) is one of the most powerful tools for this purpose [25].

All force measurements reported here were taken for the sphere-plate geometry on an atomic force microscope (Digital Instruments Nanoscope III) using a microfabricated cantilever with integral tip and a flat silica surface. In the force mode the cantilever tip is held stationary and the flat surface is mounted on a piezoelectric tube which can be driven in a controlled manner toward and away from the tip. The cantilever spring constant was calibrated using the method of Cleveland et al. [26] and was found to be 0.038 Nm^{-1}. The AFM fluid cell and the silica wafer were thoroughly washed in a strong alkaline solution. The cantilever and silica wafer were ultraviolet irradiated for 30 min (9 $mWcm^{-2}$ at 253.7 nm) in a laminar flow cabinet prior to use. The effective radius of the cantilever tip was determined using the method of Drummond and Senden [27] and was found to be 150 nm. The force measurements were made using solutions of the poly(acrylic acid) of known concentration, all at pH 10. Scanning frequencies from 0.1 to 0.5 Hz were used over

scan ranges of 0–100 nm. The force curves were found to be reversible, hence only the approaching curves are shown.

In our AFM measurements the total force acting between the tip (with an effective radius of a) and flat surface was primarily composed of the electric double layer repulsion (F_R), van der Waals attraction (F_A), and depletion force (F_D). Although the interaction geometry in the AFM was between a sphere and flat plate, the Deryaguin approximation allows the geometry to be simplified to the interaction of two plane parallel half-spaces [28]. The approximation relates the interaction force between a sphere and flat surface to the interaction energy per unit area (E_{PP}) between two planar surfaces by

$$E_{pp} = (F_R + F_A + F_D)/(2\pi a) \quad (4)$$

As a result, the interaction energy derived from Eq. (4) can, to a first approximation, be used as a qualitative indication of the interaction energy per unit area that was acting between the latex particles in our dilute dispersions.

3. Results and discussion

Flocculation of the very dilute latex dispersions (0.002–0.007% w/w) was monitored over time using small-angle static light scattering as a function of the poly(acrylic acid) and initial particle concentrations. Fig. 2 shows the typical floc growth behaviour observed in these aggregating dispersions. It is interesting to note that floc growth continued for quite a number of hours before coming to completion. This time scale was much longer than commonly observed in polymer-induced bridging flocculation processes [9,10] or simple electrolyte-induced coagulation processes at high salt concentrations [7]. An explanation for the slow kinetics observed in the depletion flocculation processes is that depletion flocculation takes place in the secondary potential energy minimum [14]. This can be seen clearly from our atomic force microscopy data, which will be discussed further on. Although there is no repulsive energy barrier when

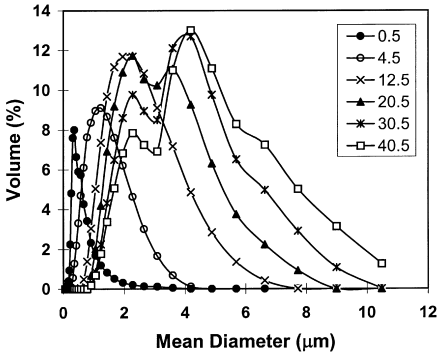

Fig. 2. Typical growth behaviour of the latex particle flocs as induced by depletion flocculation using poly(acrylic acid). The polyacid and initial particle concentrations used here are 10 g l^{-1} and 0.0035% w/w, respectively. The insert shows the flocculation time in hours.

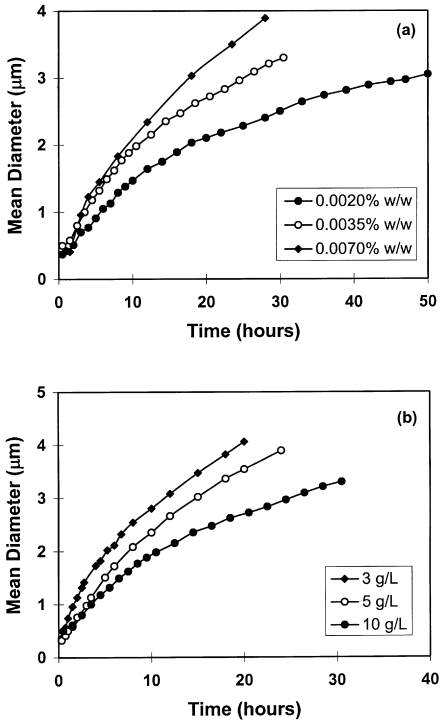

Fig. 3. Dependence of the floc growth kinetics on (a) the concentration of initial latex particles at 10 g l^{-1} poly(acrylic acid), and (b) the concentration of poly(acrylic acid) at 0.0035% w/w latex particles.

two particles approach, there is also a large probability for the interacting particles to separate under thermal motions due to the relatively shallow secondary potential energy well.

The flocculation kinetics were found to be significantly influenced by the levels of the initial particles (Fig. 3a) and the polyacid (Fig. 3b) in solution. To a first approximation, one can view aggregate formation as a simple bimolecular collision process whereby the rate of aggregate formation is proportional to the product of the rate constant and the square of particle (or cluster) concentration. It is then easy to comprehend why there would be an increase in floc growth kinetics with an increase in the initial particle concentration. However, the observed trend in the floc growth kinetics with polymer concentration (see Fig. 3b) is somewhat surprising. One would expect the growth rate to rise with an increase in polyacid concentration, since our experimental observation (vide infra Fig. 7) indicates that the secondary potential energy well deepens with increasing polymer concentration. Slower kinetics at higher polyacid concentrations must be related to the increase in solution viscosity. Rheological measurements show that an aqueous solution containing 10 g l^{-1} PAA (8.1 cP) is almost twice as viscous as a 3 g l^{-1} PAA solution (4.1 cP).

During the floc growth period the scattered intensity from each flocculating sample was seen to rise. However, once the average floc size had grown to about 10 times the primary particle size, the scattering exponent calculated from the linear portion in the fractal regime (cf. Eq. (2)) reached

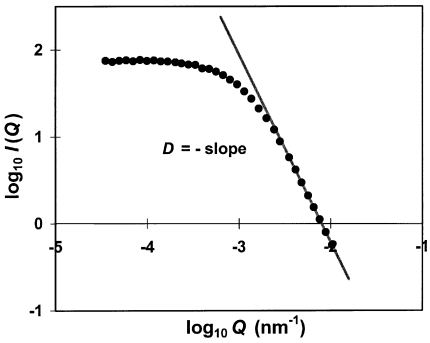

Fig. 4. A typical light scattering pattern from the depletion flocculated latex flocs. The poly(acrylic acid) and initial particle concentrations used here are 20 g l^{-1} and 0.0035% w/w, respectively.

a plateau value. This plateau value was taken to be the mass fractal dimension, *D* of the flocs in the sample. Fig. 4 shows a typical scattering pattern from which *D* was derived. It is evident that the depletion flocculated latex particles possessed typical scattering characteristics of a mass fractal object.

Fig. 5 shows that the mass fractal dimension of the latex flocs varied significantly with changes in either the polyacid or initial particle concentration, ranging from 2 up to 3. The *D* values at very low polymer concentrations are much higher than those generally obtainable from salt aggregation or polymer bridging. At a fixed particle concentration, *D* decreased as the polymer concentration was raised at low levels of the polyacid, eventually levelling off at high polymer concentrations. This trend can be better understood when results of the atomic force microscopy measurements are presented. Nevertheless, it suffices to say at this point that the determining factor for the formation of a particular floc structure is the depth of the secondary potential energy well between a pair of primary particles. The well depth will necessarily influence the efficiency of particle sticking upon collision.

At a fixed level of PAA the fractal dimension was seen in Fig. 5 to decrease as the initial particle concentration was increased. This can be attributed to the increased frequency of particle collision. The presence of a larger number of

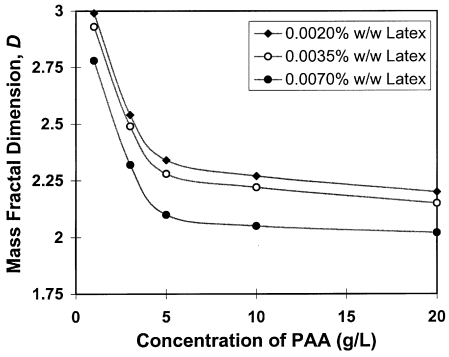

Fig. 5. Mass fractal dimension of the depletion flocculated latex flocs as a function of poly(acrylic acid) and initial particle concentrations.

particles in the flocculating sample results in a reduction in the time available for a particle attached onto the edge of a cluster to roll around in order to find its most favourable energy position prior to it being locked into position by other incoming particles. This reduced ability for particle rearrangement or cluster structural annealing gives rise to more open floc structures.

Having described the scattering results, it should be pointed out that the power-law scattering relation (i.e. Eq. (2)) is derived based on the assumption that the fractal aggregate may be treated as a Rayleigh–Gans–Debye scatterer. That is, its index of refraction should be close to that of the dispersion medium, and the phase difference between the two waves passing, respectively, through the aggregate and the solvent should be small. These conditions can generally be met for small, open aggregates. But care should be taken for aggregates with $D \gg 2$. Aggregates possessing *D* far greater than 2 are relatively compact and geometrically opaque. As a result, there may be multiple scattering and shadowing effects among the primary particles.

Lindsay et al. [29,30] have carried out qualitative and numerical analyses of the effects of multiple scattering on the scattering pattern. They conclude that multiple scattering mainly changes the mean-field index of refraction of an aggregate and hence its scattering intensity, but the power-law scattering relation is unaffected in the fractal regime (i.e. within $1/R \ll Q \ll 1/r_0$). Unfortunately, the effects of particle shadowing on the measured scattering exponent are still unknown. But we are confident that our observed trend in the mass fractal dimension as a function of the polyacid concentration is reliable, although the absolute value may be subject to some uncertainty. A very similar trend to ours has been observed in a small-angle light scattering work of Poon et al. [16] on the depletion flocculation of a concentrated PMMA particle dispersion (10% v/v) (compare Fig. 3(d) of Ref. [16]). Since their particles were dispersed in an almost optical matching solvent, shadowing or multiple scattering effects are expected to be negligible.

To help understand the observed floc structural behaviour in our scattering study, the forces between two solid surfaces in the presence of varying concentrations of the non-adsorbing poly(acrylic acid) were measured on an atomic force microscope; the results of which are illustrated in Fig. 6. Since these force curves have been normalised by the effective radius of the cantilever tip, they possess the same features as the corresponding potential energy curves per unit area between two planar surfaces (the Deryaguin approximation). Values calculated from the AFM data for the depth of the secondary potential energy well are shown in Fig. 7. Three important features regarding the data in Fig. 6 and Fig. 7 are worth mentioning: (a) In the presence of the non-adsorbing polyacid there exists a shallow secondary potential energy minimum between two solid surfaces. The electrostatic repulsive energy barrier is by comparison very significant. This clearly indicates that depletion flocculation is indeed a secondary potential energy

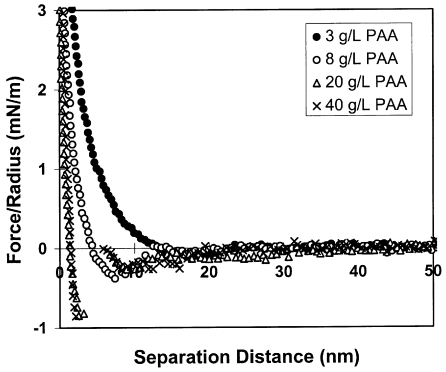

Fig. 6. The normalised force curves between the AFM cantilever tip and silica wafer as a function of poly(acrylic acid) concentration.

minimum process; (b) As the polyacid concentration is increased, the secondary energy well deepens. This is accompanied by the displacement of the secondary energy well toward smaller interparticle separation distances and also a decrease in the electrostatic repulsive energy barrier; and (c) Above 20 g l^{-1} polyacid the depth of the secondary energy well remains essentially unchanged.

As mentioned in the Introduction, a common consequence with increasing polymer concentration is an increase in the solution osmotic pressure which is accompanied by a decrease in the polymer size (i.e. the depletion layer thickness near the particle surface). Higher osmotic pressures at increased polymer concentrations are certainly one of the driving forces behind the observed deepening in the secondary energy well, whereas smaller depletion layer thickness can partly account for the movement in the position of the well minimum toward smaller surface separation distances. Since poly(acrylic acid) in a solution of pH 10 is expected to be highly charged, an increase in the polyacid concentration will lead to a noticeable increase in the solution ionic strength. This will result in a compression of the Debye decay length in the diffuse part of the electric double layer surrounding a charged surface. Ionic strength is thus another contributing factor for the observed force (or energy) behaviour in Fig. 6.

Although not shown here, fitting results of the measured force curves using the appropriate force equations show that both the size of the polymer coil and the Debye decay length around the charged surfaces became very small and relatively insensitive to polymer concentration at high polyacid levels. Under these conditions any increase in the depletion attraction energy due to increased solution osmotic pressure was offset by the electrostatic repulsion. Clearly, the observed behaviour in Fig. 6 was the result of a complex interplay between the osmotic pressure, depletion layer thickness and ionic strength effects.

The AFM results provide solid information for explaining qualitatively the trend in the floc fractal dimension with varying levels of the polyacid (cf. Fig. 5). An increase in the polymer concentration results in the deepening of the secondary potential energy well and hence a higher particle sticking efficiency. The increased probability of particle sticking upon collision prevents a particle from reaching further into the interior of the existing cluster structure or rearranging on the cluster surface. The result will be a more open floc structure with a lower mass fractal dimension. The levelling off of the fractal dimension simply corresponds to the plateau in the depth of the secondary energy well.

We have so far been focussed on the structural compactness of depletion-induced flocs. Another important property that has close relevance to industrial applications is the mechanical strength of a floc. Tadros and his coworkers [21–24] have published a series of papers on this subject. They found that concentrated dispersions with added non-adsorbing polymer exhibited Bingham yield stress behaviour. The magnitude of this yield stress was strongly dependent on the polymer and particle concentrations.

In this work, the Bingham yield stress was obtained at a range of poly(acrylic acid) concentration (0–1 g l^{-1}) and latex particle concentration (15–30% w/w). The results are shown in Fig. 8. Below 0.05 g l^{-1} PAA the yield stress was found to be similar to that of the dispersion without PAA. As commonly observed, the Bingham yield stress increased as the polymer concentration was raised. Interestingly, here the yield stress reached a saturation level at high polymer

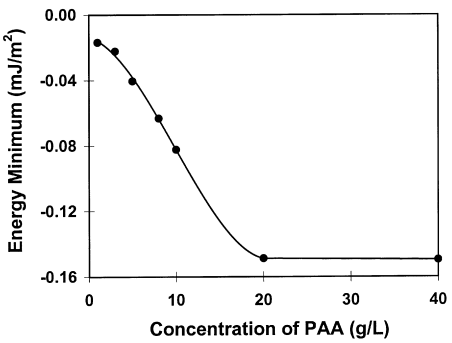

Fig. 7. Dependence of the depth in the secondary potential energy well between two planar surfaces on the poly(acrylic acid) concentration.

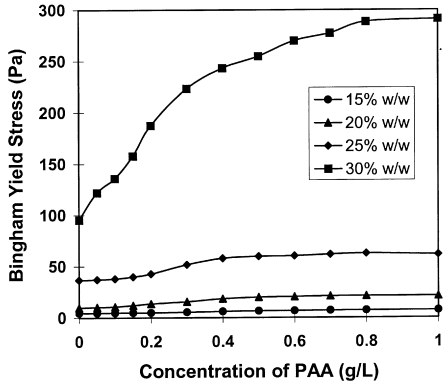

Fig. 8. Dependence of the floc Bingham yield stress on the concentrations of poly(acrylic acid) and latex particles.

Table 1
The coordination numbers, *n*, used in the calculation of energy of separation under various poly(acrylic acid) and latex particle concentrations

	Concentration of PAA (g l^{-1})										
Latex concentration	0.05	0.1	0.15	0.2	0.3	0.4	0.5	0.6	0.7	0.8	1.0
15% w/w	–	12	6.9	6	5.2	3.8	2.6	1.9	1.9	1.9	1.9
20% w/w	12	6.9	6	5.2	3.8	2.6	1.9	1.9	1.9	1.9	1.9
25% w/w	12	6.9	6	5.2	3.8	2.6	1.9	1.9	1.9	1.9	1.9
30% w/w	12	6.9	6	5.2	3.8	2.6	1.9	1.9	1.9	1.9	1.9

concentrations. Furthermore, the yield stress was strongly influenced by the solids concentration in the sample, decreasing rapidly as the particle concentration was lowered.

Values of the Bingham yield stress can be used to estimate the energy (E_{sep}) required to separate the flocs into single units via Eq. (3). In this equation the only unknown is the number of contacts per particle inside a floc (i.e. the coordination number, *n*). For a face-centred cubic crystallite n=12, whereas the generally tenuous nature of a mass fractal aggregate normally gives rise to low *n* values. In this work *n*, as a function of the polyacid concentration, was generated from the trend of the measured mass fractal dimensions of Fig. 5. We are aware that the data in Fig. 5 are, strictly speaking, only applicable to very dilute dispersions. Nevertheless, a similar trend to that of Fig. 5 has been reported for concentrated non-aqueous dispersions of coated PMMA particles [16].

In our calculation of *n* a value of D=3 was assumed for polyacid concentrations close to the phase stability boundary. For polymer concentrations corresponding to the plateau region in the Bingham yield stress curves a value of D=1.8 was used. In this region it is expected that diffusion-limited cluster-cluster aggregation prevails [16] and hence the fractal dimension should be close to the commonly recognised values of 1.75–1.80 [3,7]. In the slope region a linear relation was used to interpolate the *D* values. We believe that the above approach used in estimating the coordination number is closer to reality. Nevertheless, qualitative features in the estimated separation energy curves will remain the same even if a constant value of *D* or *n* is used for the varying levels of polymer.

The *n* value corresponding to a particular *D* is estimated following the method of Torres et al. [31]. The number of particle centres, $N(r)$, within a radius of *r* of a given particle in a floc is given by Eq. (5),

$$N(r) = 1 + H(r-2r_0)B(r/r_0)^D \quad (5)$$

where $H(r-2r_0)$ is the Heaviside step function, which accounts for the excluded volume. From this equation it can be shown that the number of nearest neighbours is given by

$$n = B2^D \quad (6)$$

where *B* is the structure pre-factor and is a function of *D*. Various approaches can be taken to estimate *B*. For convenience, use was made of the *B*–*D* curve as given by Gmachowski [32] from calculations of computer simulated aggregates. The *n* values used for the calculation of energy of separation (E_{sep}) are tabulated in Table 1. The estimated E_{sep} data are shown in Fig. 9.

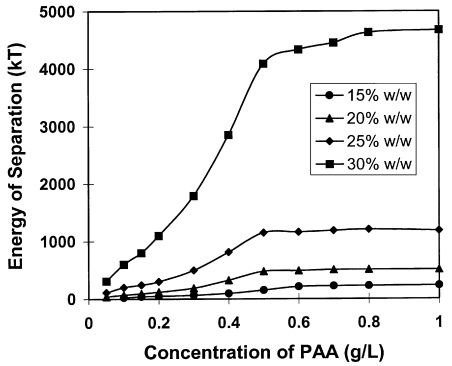

Fig. 9. Energy required to break the latex flocs into single units as a function of poly(acrylic acid) and initial particle concentrations.

As can be seen from Fig. 9, as the polymer concentration was raised, the attraction between the primary particles increased, but it eventually reached a plateau value at high polymer concentrations. Therefore, the trend in the strength (τ_B) of the latex flocs with varying concentrations of the polyacid was seen to follow closely that in the magnitude of the energy required to break the interparticle bonds. Although the coordination number (*n*) decreased from 12 to 1.9 as the polyacid concentration was increased, nE_{sep} still had a marked increase. There was also a significant increase in the energy required to break the flocs when the initial particle concentration was raised.

To sum up we have observed that the structural compactness and strength of the depletion-induced latex flocs were strongly dependent on the levels of the polyacid. The underlying factor that led to the observed behaviour is the energy that acts among the primary particles.

4. Conclusions

Small-angle static light scattering and rheometry have been utilised to explore, respectively, the structure and strength of polystyrene latex particle flocs that were formed by adding a non-adsorbing poly(acrylic acid). It was found that both the structural compactness and strength of the

latex flocs were highly influenced by the polyacid concentration, as well as the initial concentration of the primary particles. In particular, the polymer concentration effect on the floc structure and strength can be qualitatively explained by knowledge of the interparticle interaction energy that was either directly obtained from atomic force microscopy measurements or estimated from the Bingham yield stress. This work shows clearly that the fundamental floc characteristics are ultimately controlled by the interaction forces that act between the primary particles.

One of the important findings of this study is that dense aggregates can be obtained through the depletion flocculation mechanism. This is mainly attributed to the fact that depletion flocculation only takes place in the secondary potential energy well. Although there is no energy barrier for two particles to approach each other, the probability for the sticking particles to escape the secondary energy well is also relatively high. As a result, particles will have to collide many times before permanently sticking to each other. Hence a particle can penetrate deeper into the interior of a cluster prior to being intercepted by the arms of the cluster. In essence, depletion flocculation can be viewed as a diffusion-limited process with large reversibility.

Acknowledgements

The authors wish to acknowledge the support of the Centre for Multiphase Processes, a Special Research Centre of the Australian Research Council.

References

[1] B.M. Moudgil, S. Behl, in: K.A. Matis (Ed.), Flotation Science and Engineering, Marcel Dekker, New York, 1995.
[2] E.J.W. Verwey, J.Th.G. Overbeek, Theory of the Stability of Lyophobic Colloids, Elsevier, New York, 1948.
[3] M.Y. Lin, H.M. Lindsay, D.A. Weitz, R. Klein, R.C. Ball, P. Meakin, J. Phys. Condens. Matter 2 (1990) 3093.
[4] M.Y. Lin, H.M. Lindsay, D.A. Weitz, R.C. Ball, R. Klein, P. Meakin, Phys. Rev. A 41 (1990) 2005.
[5] R.J. Hunter, Foundations of Colloid Science, vol. 1, Oxford University Press, London, 1987.
[6] B.B. Mandelbrot, The Fractal Geometry of Nature, Freeman, San Francisco, CA, 1982.
[7] J.L. Burns, Y.-D. Yan, G.J. Jameson, S. Biggs, Langmuir 13 (1997) 6413.
[8] K. Wong, B. Cabane, R. Duplessix, J. Colloid Interface Sci. 123 (1988) 466.
[9] S. Biggs, M. Habgood, G.J. Jameson, Y.-D. Yan, Separation Purification Technology (2000), in press.
[10] S.W. Glover, Y.-D. Yan, G.J. Jameson, S. Biggs, Separation Purification Technology (2000), in press.
[11] R. Jullien, R. Botet, P.M. Mors, Faraday Discuss. Chem. Soc. 83 (1987) 125.
[12] S. Stoll, J. Buffle, J. Colloid Interface Sci. 205 (1998) 290.
[13] R. Li-in-on, B. Vincent, F.A. Waite, ACS Symp. Ser. 9 (1975) 165.
[14] P. Jenkins, M. Snowden, Adv. Colloid Interface Sci. 68 (1996) 57.
[15] S. Asakura, F. Oosawa, J. Chem. Phys. 22 (1954) 1255.
[16] W.C.K. Poon, A.D. Pirie, P.N. Pusey, Faraday Discuss. Chem. Soc. 101 (1995) 65.
[17] J.L. Burns, Y.D. Yan, G.J. Jameson, S. Biggs, Prog. Colloid Polym. Sci. 110 (1998) 70.
[18] J.W. Goodwin, J. Hearn, C.C. Ho, R.H. Ottewill, Colloid Polym. Sci. 252 (1974) 464.
[19] A.L. Stone, D.F. Bradley, J. Am. Chem. Soc. 83 (1961) 3627.
[20] J. Teixeira, J. Appl. Cryst. 21 (1988) 781.
[21] D. Heath, Th.F. Tadros, Faraday Discuss. Chem. Soc. 76 (1983) 203.
[22] C. Prestidge, Th.F. Tadros, Colloids Surf. A 31 (1988) 325.
[23] Th.F. Tadros, Langmuir 6 (1990) 28.
[24] Th.F. Tadros, A. Zsednai, Colloids Surf. A 49 (1990) 103.
[25] V.S.J. Craig, Colloids Surf. A 129-130 (1997) 75.
[26] J.P. Cleveland, S. Manne, D. Bocek, P.K. Hansma, Rev. Sci. Instr. 64 (1993) 403.
[27] C.J. Drummond, T.J. Senden, Colloids Surf. A 87 (1994) 217.
[28] J. Israelachvili, Intermolecular and Surface Forces, 2nd edition, Academic Press, San Diego, CA, 1991.
[29] H.M. Lindsay, M.Y. Lin, D.A. Weitz, P. Sheng, Z. Chen, R. Klein, P. Meakin, Faraday Discuss. Chem. Soc. 83 (1987) 153.
[30] Z. Chen, P. Sheng, D.A. Weitz, H.M. Lindsay, M.Y. Lin, P. Meakin, Phys. Rev. B 37 (1988) 5232.
[31] F.E. Torres, W.B. Russel, W.R. Schowalter, J. Colloid Interface Sci. 142 (1991) 554.
[32] L. Gmachowski, J. Colloid Interface Sci. 178 (1996) 80.